Comput Geosci (2007) 11:275–281
DOI 10.1007/s10596-007-9051-0

ORIGINAL PAPER

Utilisation of the image analysis method for the detection of the morphological anisotropy of calcite grains in marble

Boguslaw Obara · Alena Kožušníková

Received: 14 July 2006 / Accepted: 19 April 2007 / Published online: 22 May 2007

Abstract This paper presents the development and utilisation of an automated image processing algorithm for detection and analysis of grains. Using optical polarising microscopy, a set of colored images are collected from an area on a thin section. A filtering operation, using rotation of a morphological alternating sequence filter (based on a structuring element), is used to remove twinning features within individual grains. Filtering is followed by the watershed segmentation technique to determine grain boundaries. The method is used for the identification of calcite grains in marble and the subsequent analysis of morphological anisotropy.

Keywords Grain boundaries · Image processing and analysis · Microscopy · Morphological anisotropy · Rock structure

1 Introduction

1.1 Rock anisotropy

One of the important factors that determine the behaviour of rocks is their anisotropy. The influence of rock anisotropy was investigated especially from the standpoint of strength properties (e.g. [1–6]), ultrasonic wave velocity [7], acoustic emission [8] and magnetic properties [7]. Anisotropy influences other physical properties as well – for instance, elastic, heat (thermal conductivity, specific heat capacity, dilatation) and transport (permeability) properties [9].

Anisotropy of rock physical properties is derived from macro- and microstructural anisotropy, which results from the geologic history of the sample. Macroscopic anisotropy is principally caused by laminar (planar) structure (e.g. bedding planes, foliation, lamination, cleavage, joint systems). Microscopy anisotropy includes priority orientation of rock minerals, arrangement and orientation of fabric defects and boundaries between crystal grains, twinning planes and primary microfissures. The anisotropic features depend upon specific rock genesis (e.g. [2]).

Preferred morphological and optical orientation of minerals is an attribute for most metamorphic rocks. Such orientation is often visible during macroscopic study. Determination of the optical orientation of specific minerals is necessary to execute special microscopy analysis by means of Fjodorov's stage [10]. Marble is quasi-monomineral metamorphic rock that is made up of an aggregate of calcite crystal grains. The preferred orientation of calcite in marble is often expressively developed. In particular, (0112) twinning and (1011) translational gliding occur during the plastic deformation of marble (Fig. 1).

The structural and mechanical properties of marble under various conditions of pressure, temperature and chemical solution were studied by Lepper [12], Griggs et al. [13], Turner et al. [14], Handin et al. [15] and Royer-Carfagni [16]. Previous studies show that Yule marble is characterised by a certain systematic arrangement of the ellipsoidal grains of calcite. In [12] it has been shown that the strength of the marble perpendicular to the planes of

B. Obara (✉)
Strata Mechanics Research Institute, Polish Academy of Sciences,
Reymonta 27,
Krakow PL 30-059, Poland
e-mail: ngobara@cyf-kr.edu.pl

A. Kožušníková
Institute of Geonics, Academy of Sciences of the Czech Republic,
Studentská 1768,
Ostrava-Poruba 708 00, Czech Republic
e-mail: kozusnik@ugn.cas.cz

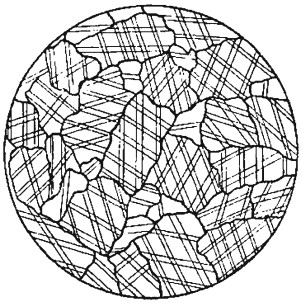

Fig. 1 Schematic microscopic structure of marble – grains with twinning according (0112) [11]

"grains" is nearly 1.5-fold greater than the strength determined parallel to the planes. Stiffness parallel to the preferential planes is greater; the relation between the corresponding values of the modulus of elasticity ($E_{//}/E_{\perp}$) was approximately 1.6.

Petrofabric measurements can provide considerable information concerning the preferred grain boundary directions. In particular, such measurements made by image analysis are made faster and are therefore more useful for statistical analysis than manual analysis. Therefore, the method of image analysis was chosen for the determination of the morphological preferred orientation of calcite.

1.2 Image analysis of rock structure

Image processing and analysis are very powerful tools when morphological information is required to understand the behaviour of rocks. Utilisation of image analysis methods allows displaying the most diverse features of rock structures: grains (grain boundaries; e.g. [17]) and microcracks (e.g. [18]).

Image analysis applied to rock structure can be divided into three main steps:

- image acquisition
- "noise" reduction/elimination and image segmentation
- feature extraction and characterization (via parameters or functions).

Table 1 Thermal dilatation (arranged according to [24])

Measurement in axis	Thermal expansion in heating rank 25°–1000°C	Thermal expansion in cooling rank 1000°–25°C	Permanent dilatation
	%	%	%
x	4.51	−2.72	1.79
y	2.24	−1.43	0.81
z	1.99	−1.38	0.61

During such analysis, the problem of the statistical and stereological nature of rock has to be solved. In the case of the analysis of the morphological preferred orientation of calcite, we have to be focussed on the identification of grains. The elimination of twinning is necessary for the image analysis of calcite grains and the determination of their preferred morphological orientation.

Several image analysis methods have been used for the segmentation and analysis of grains in images obtained from microscopy. Mlynarczuk [19] proposed an algorithm based on the watershed method [29] for segmenting grains in polarizing microscope images of dolomite and quartzite. Luumbreras and Serrat [20] utilized a grey-scale-based, region-merging algorithm for segmentation in microscopy images of thin sections of marble. Zhou et al. [21] developed the method of RGB colour image segmentation of mineral grains in petrographic images by utilising edge and region data. In [22], digital image analysis methods were proposed for the determination of the mortar aggregate/binder ratio and grading curve on the basis of observations performed on thin sections; thus, combining digital image analysis methods and HSI/RGB colour models with standard optical techniques. Grain boundary detection, based on gradient filtering, was presented by Heilbronner [17]. The proposed procedure made use of multiple input images: sets of regularly polarised micrographs and orientation/disorientation images. Ross et al. [23] have addressed the grain identification problem using a specialized branch of evolutionary computation called genetic programming.

The presented paper shows the results of the research on the development and utilisation of image processing and analysis algorithms for the automatic determination of the morphological preferred orientation of marble.

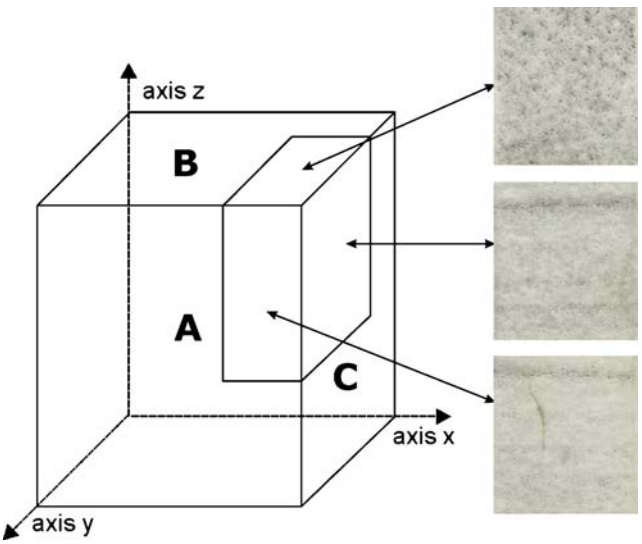

Fig. 2 Location of thin sections in marble sample and the orientation of axis

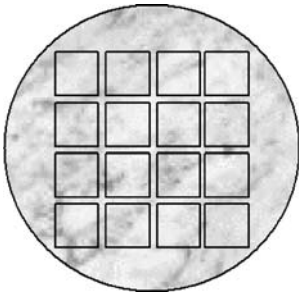

Fig. 3 Distribution of measurement fields on thin sections

2 Tested material and anisotropy of physical properties

The marble samples tested are from the Horni Lipova quarry (Jeseniky Mts, Czech Republic). The marble is composed largely of calcite, with relatively few impurities–muscovite, graphite, iron oxides and, in isolated cases, pyrite crystals.

The anisotropy of strength was not expressive, but the elastic modulus parallel to the foliation was measured to be 1.2 times the elastic modulus perpendicular to the foliation. The ratio between the corresponding values of ultrasonic wave velocity ($v_{p//}/v_{p\perp}$) was 1.06. The most expressive anisotropy was discovered to be thermal dilatation (Table 1). Thermal dilatation was measured by using the thermo-mechanical analyser SETARAM over a temperature range from 20° to 1,000°C and back. The tested samples were 7×7×7 mm cubes. Expansion was measured in all three directions.

3 Preparing and evaluation of thin sections

Thin sections from the marble were observed under an AXIOPLAN-ZEISS polarisation microscope (Fig. 2) with a

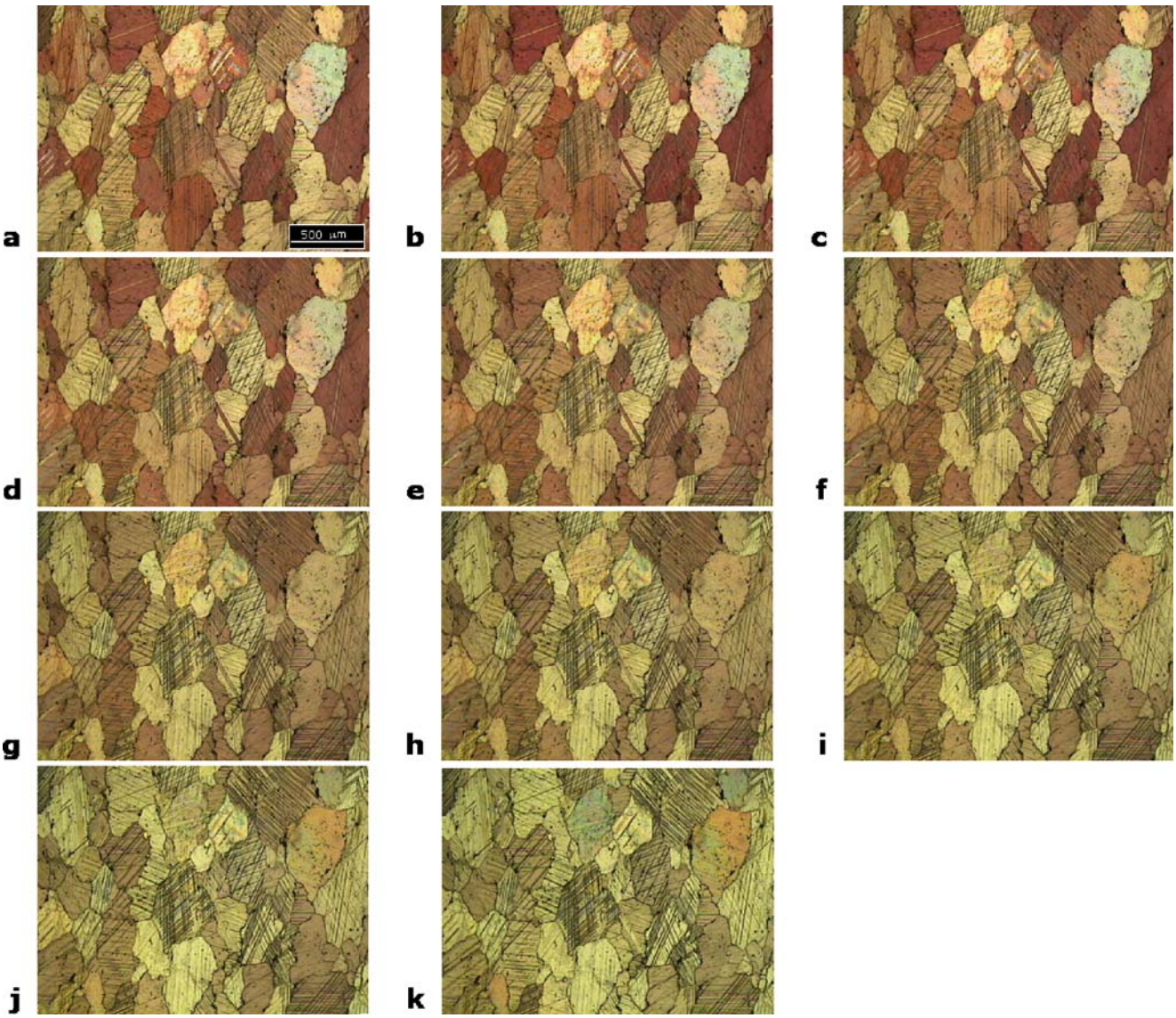

Fig. 4 Selected measurement field of marble structure: 11 images taken with two crossed nicols

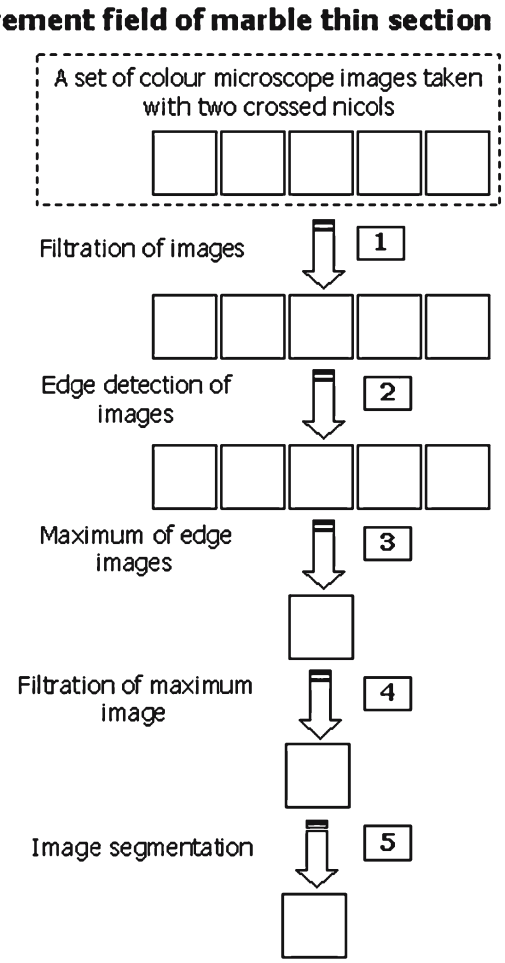

Fig. 5 The scheme of main parts of grain's segmentation procedure based on set of colour images of one measurement field taken with two crossed nicols

JVC TK-C1381 CCD camera connected via a MATROX MERVELL G200 video card to a PC. The polarisation system uses two nicols: one is fixed in place and the other can be rotated [25], while the thin section is kept firmly in place. Several measurement areas are selected on each thin section (Fig. 3). Eleven color images were taken on each area using crossed nicols, each at a different cross angle (Fig. 4).

Each grain in a thin marble section has its own preferred direction, which is usually different from the neighbouring grains. Therefore, when we change the angle between the analyser and polariser in a polarisation microscope, each grain exhibits a different, characteristic pattern of intensity variation or incident light transmission. By rotating one nicol (16° per step), we increase the amount of information about the grain colour – see the captured sequences of images from one measurement field (Fig. 4). From the image analysis standpoint, additional colour information is very useful for the accurate segmentation of rock structure images.

Each image is 1,531×1,167 μm in size and is digitalised into 742×556 pixel resolution. There are 16.7 million colours in the RGB colour system. These images analysed using the grain segmentation process described in the sections below.

4 Extraction of features and image segmentation

4.1 Image analysis procedure

The scheme for grain segmentation, using the color images derived from each measurement area, is shown in Fig. 5. Grain segmentation has three general steps:

– noise reduction. For example, this may consist of median filtering as in [17], or dilation/erosion by reconstruction as in [19];
– edge detection. For example, Canny edge detection as in [26], Sobel filtering as in [17] or by morphological gradient as in [19];
– segmentation. For example, region-merging [20], skeletonisation [17, 26] or the watershed method [19].

Our specific choices for these steps are addressed in Filtering and Imaging segmentation. The most important part of the segmentation procedure in our study is the noise reduction step. From the point of view of image analysis, twinning planes within grains look similar to microcracks – these need to be distinguishable from grain boundaries for satisfactory segmentation. We utilize the idea of Obara [18, 27, 28], which uses a rotated linear structuring element to reduce the influence of microcracks.

4.2 Filtering

The filtering procedure is based on using a rotated stencil consisting of two linear structuring elements that are defined in perpendicular directions. An exemplary of structuring element is presented in Fig. 6. The structuring elements is rotated every 15° (0°, 15°, 30°, 45°, ..., 165°).

Fig. 6 Proposed structuring element with a size of 6 pixels.

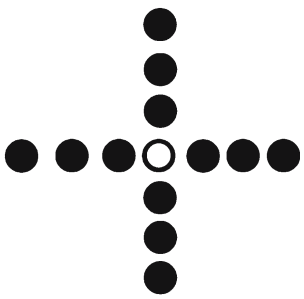

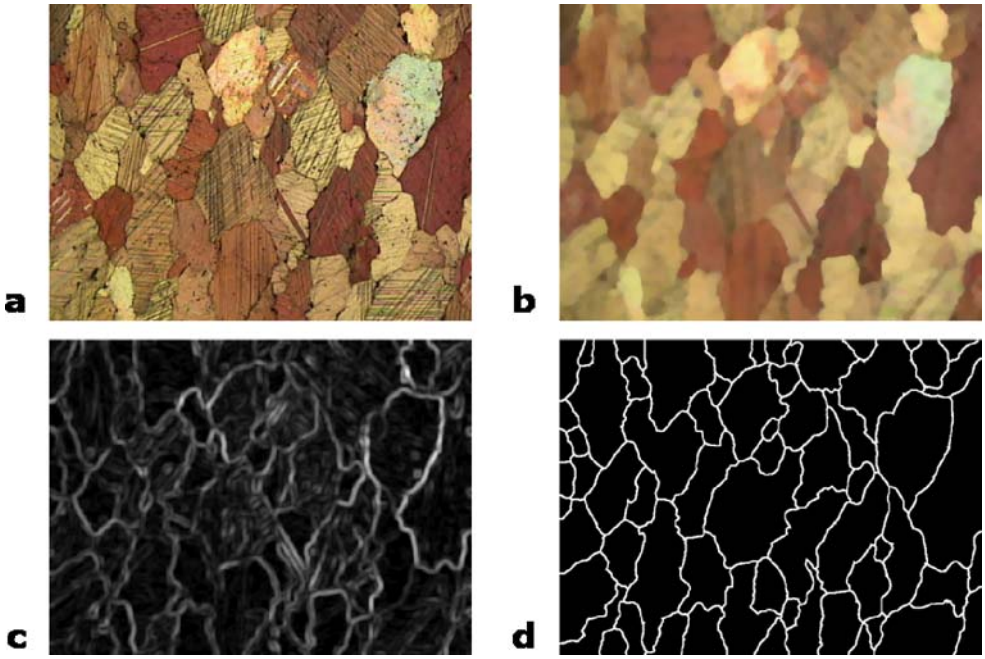

Fig. 7 Grains segmentation procedure: a) one of input images, b) one of filtered images, c) maximum image of 11 morphological gradients of 11 filtered images, d) segmented grains

The filtering procedure is completed by the use of alternate sequential filtering (ASF) [29] using the proposed structuring elements. Equations (1) and (2) show the definition of the alternate sequential filtering.

If filters C_i and O_i satisfy the three conditions shown below:

$$\left.\begin{array}{r} C_i - increasing\ with\ i, \\ O_i - decreasing\ with\ i, \\ O_1 \le C_1, \end{array}\right\} \Leftrightarrow \ldots O_n \le \ldots \le O_2 \le O_1 \le C_1 \le C_2 \le \ldots \le C_n \ldots \quad (1)$$

We can construct alternate sequential filter [29]:

$$M_i = C_i O_i \ldots C_2 O_2\ C_1 O_1 \quad (2)$$

This ASF consists of alternating openings (O_i) and closings (C_i) of increasing size i. The size of each structuring element increases by one each iteration i from 1 to 8.

The point of a closing and opening combination is that it removes a specific type of noise, which depends on the shape of the structuring element. The reason for the sequence of increasing size shapes is to eliminate such noise up to a certain size (in the order of smallest to largest).

Such filtering with the proposed structuring element enables us to decrease the influence of twinning on the grain segmentation process.

4.3 Image segmentation

Eleven colour images (Fig. 7a) of each measurement field are filtered by using the alternate sequential filter (Fig. 7b). The image of the maximum values of 11 morphological gradients of the filtered images is then calculated (Fig. 7c). The maximum image is filtered using a filter based on open and close by the reconstruction. Then regional minimums of the filtered image are calculated. The image contains the regional minimums that are used in the watershed segmentation technique (Serra, 1982). The final stage of grain segmentation processes is shown in Fig. 7d.

The image processing and analysis algorithm was developed in Aphelion ADCIS software (see Appendix B) and used for the segmentation of the microscope images of

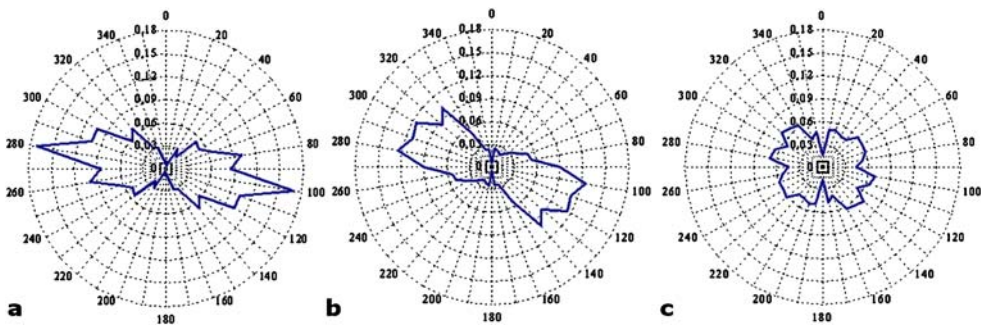

Fig. 8 Feret angle rose diagram of segmented grains in thin section: a), b) and c)

marble. The full code of the algorithm is presented in Appendix A. The computation time of a set of 11 images for one measurement field takes 4 s on a standard PC computer (2 GHz processor, 1 GB RAM).

5 Measurement of morphological anisotropy

Most by the measurements performed on a set of grains (e.g. Feret diameter) are meaningless for those grains that cut the border of the image. Therefore, removing the grains that cut the image border is a prerequisite for the measurement.

To measure out the morphological preferred orientation of calcite, we consider the Feret angle analysis of all the segmented images of the marble structure. The Feret angle was measured from axis z on a thin section A and C, and from axis y on thin section B.

For all the full grains identified on A, B and C thin sections, the Feret angles were calculated and the results are presented in Fig. 8.

6 Discussion

The shape factor, determined as the ratio of D_{min} (the length of the shorter side of the minimum bounding rectangle) to D_{max} (the length of the longer side of the minimum bounding rectangle) of calcite grains in thin section B is 0.79; the shape factor of calcite grains in thin section A and C is very similar – 0.58, 0.59. This indicates that the calcite grains in thin sections A and C are more elongated.

The preferred grain boundaries orientation is different in all the thin sections. The most noticeable preferred morphological orientation of calcite grain is in thin section A (one evident peak in the rose diagram at 100°)–see Fig. 8a. The less noticeable preferred orientation of calcite grain is in thin section C (inexpressive peak in the rose diagram between 100° and 140°)–see Fig. 8b, and in the thin section B the preferred orientation of calcite grain is not visible at all (Fig. 8c).

These facts agree with the measurements of thermal dilatation. The lowest dilatation was recorded in the direction of axis z (between planes B and B), perpendicular to the foliation (see Table 1). Dilatation in direction x, y (between planes C and C, A and A) is different as well. The differences of thermal expansion are obviously caused by different preferred orientations of elongated calcite grains.

7 Conclusions

The accurate and rapid detection of grains in rock structure observed under the microscope is important from a geosciences point of view (particularly, in petrography and stereology). The proposed method allows a fully automatic grain segmentation and fast analysis of the morphological preferred orientation. The newly developed algorithm may facilitate and expedite the petrographical and stereological analysis of rock structure.

Acknowledgements This study is financially supported by the State Committee for Scientific Research of Poland through the statutory research fund, by the Grant Agency of Czech Republic – project No. 105/04/1019, by the Academy of Sciences of the Czech Republic – project AVOZ 30860518 "Physical and environmental processes in the lithosphere induced by anthropogenic activities" and by project number NP29 between the Strata Mechanics Research Institute PAS and the Institute of Geonics CAS.
The manuscript was greatly improved by the comments and suggestions made by Prof. P. Martinec.

Appendix A

Algorithm 1 Marble–grains' segmentation algorithm

```
Grains (C_IN[w], B_OUT)
{
        //-------------------------------------------------------------------------
        For(i=1; i<=w; i++)
        {
                For(j=1; j<=n; j++)
                {
                        k1=j*PI/n;
                        ASF (C_IN[i], C1[j], l(s1, k1));
                        k2=j*PI/n+PI/2;
                        ASF (C1[j], C2[j], l(s1, k2));
                        k3=j*PI/n+PI/4;
                        ASF (C_IN[i], C3[j], l(s1, k3));
                        k4=j*PI/n+3*PI/4;
                        ASF (C3[j], C4[j], l(s1, k4));
                        Blend (C2[j], C4[j], C5[j], 0.5);
                };
                Minimum (C5[1], C5[2], C6[i]);
                For(j=3; j<=n; j++)
                        Minimum (C5[j], C6[i], C6[i]);
        };
        //-------------------------------------------------------------------------
        For(i=1; i<=w; i++)
                Gradient (C6[i], C7[i], ds2);
        Maximum (C7[1], C7[2], C8);
        For(i=3; i<=w; i++)
                Maximum (C7[i], C8, C8);
        //-------------------------------------------------------------------------
        ColourToRGB (C8, G1, G2, G3);
        Maximum (G1, G2, G4);
        Maximum (G3, G4, G4);
        //-------------------------------------------------------------------------
        Close_R (G4, G5, ds3);
        Open_R(G5, G6, ds3);
        Close_R (G6, G7, ds4);
        Open_R (G7, G8, ds4);
        Close_R (G8, G9, ds5);
        Open_R (G9, G10, ds5);
        Regional_Minima (G10, B1);
        Invert (B1, B2);
        Multiply (G10, B2, G11);
        Watershed (G11, B_OUT);
        //-------------------------------------------------------------------------
        Return B_OUT;
};
```

Where:
C_IN[]–set of input images,
B_OUT–output image,
C–colour image, C[]–array of colour's images,
G–grey image, G[]–array of grey's images,
B–binary image,
n–number of filtrating directions,
w–number of images for one measurement field,
ASF (a, b, $l_{(s,\ k)}$)–alternative sequential filtering of image a on image b by linear structuring element with s size and k direction,
Gradient (a, b, d_s) – morphological edge detection of image a on image b by disk structuring element with s size,
ColourToRGB (a, b, c, d) – convert colour image a to b, c, d grey images,
Close_R (a, b, d_s) – close by reconstruction of image a on image b by disk structuring element with s size,
Open_R (a, b, d_s) – open by reconstruction of image a on image b by disk structuring element with s size,
Maximum (a, b, c) – maximum of images a and b on image c,
Minimum (a, b, c) – minimum of images a and b on image c,
Blend (a, b, c, x) – combination of a and b images with a constant x blend factor,
Regional_Minima (a, b) – regional minima of image a on image b,
Invert (a, b) – invert image a on image b,
Multiply (a, b, c) – multiply a and b images on c image,
Watershed (a, b) – "watershed" segmentation of image a on image b.

Appendix B

Software packages used:
AphelionTM v.3.0: image processing and quantitative image analysis package from ADCIS http://www.adcis.net/Products/Aphelion/GeneralDescription.html.

References

1. Colak, K., Unlu, T.: Effect of transverse anisotropy on the Hoek–Brown strength parameter 'm_i' for intact rocks. Int. J. Rock Mech. Min. Sci. **41**, 1045–1052 (2004)
2. Kwaśniewski, M.A.: Mechanical behaviour of anisotropic rocks. In: Hudson, J.A. (ed.) Comprehensive Rock Engineering, Principles, Practice & Projects, vol.1, pp. 285–312. Pergamon Press, Oxford New York Seoul Tokyo (1993)
3. Martinec, P., Keclík, L.: K metodice zjišťování vztahu strukturní a mechanické anizotropie hornin. Geol. Průzk. **XVII**(9), 256–269 (1975)
4. Ochocińska, T.: Anizotropia wytrzymalosci na jednoosowe sciskanie i rozrywanie cechsztynskich anhydrytow z rejonu Polkowice. Arch. Min. Sci. **25**(2), 233–247 (1980)
5. Přikryl, R.: Some microstructural aspects of strength variation in rocks. Int. J. Rock Mech. Min. Sci **38**, 671–682 (2001)
6. Ramamurthy, T.: Strength and modulus responses of anisotropic rocks. In: Hudson, J.A. (ed.) Comprehensive Rock Engineering, Principles, Practice & Projects, vol.1, pp. 313–329. Pergamon Press, Oxford New York Seoul Tokyo (1993)
7. Štelcl, J., Beneš, K., Pták, J.: Základy drobné tektoniky a petrotektoniky. Masarykova Univerzita, Brno (1980)
8. Přikryl, R., Lokajíček, T., Li C., Rudajev, V.: Acoustic emission characteristics and failure of uniaxially stressed granitic rocks: the effect of rock fabric. Rock Mech. Rock Eng. **36**(4), 255–270 (2003)
9. Franklin, J.A., Dusseault, M.B.: Rock engineering. McGraw-Hill Publishing Company, New York (1989)
10. Hejtman, B.: Petrografie metamorfovaných hornin. Nakladatelství ČSAV, Praha (1962)
11. Slavík, F., Novák, J., Kokta, J.: Mineralogie. Academia, Praha (1974)
12. Lepper, H. A. Jr.: Compression tests on oriented specimens of Yule marble. Am. J. Sci. **247**, 570–575 (1949)
13. Griggs, D., Miller, W.B.: Deformation of Yule marble: Part 1. Geol. Soc. AmEr. Bull. **62**, 853–862 (1951)
14. Turner, F. J., Griggs, D.T., Heard, H.C.: Experimental deformation of calcite crystals. Geol. Soc. Amer. Bull. **65**, 883–934 (1954)
15. Handin, J, Higgs, D, O'Brien, J.K.: Torsion of Yule marble under confining pressure. Geological Society of America Memorials **79**, 245–274 (1960)
16. Royer-Carfagni, G.F.: On the thermal degradation of marble. Rock Mech. Min. Sci **36**, 119–126 (1998)
17. Heilbronner, R.: Automatic grain boundary detection and grain size analysis using polarization micrographs or orientation images. J. Struct. Geol. **22**, 969–981 (2000)
18. Obara, B.: Identification of transcrystalline microcracks observed in microscope images of dolomite structure using image analysis methods based on linear structuring element processing. Comput. Geosci. **33**(2), 151–158 (2007)
19. Młynarczuk, M.: Some remarks on the application of image analysis and image processing for the description of the geometrical structures of rock. Fizykochem. Probl. Mineral. **33**, 107–116 (1999)
20. Luumbreras, F., Serrat, J.: Segmentation of petrographical images of marbles. Comput. Geosci. **22**, 547–558 (1996)
21. Zhou, Y., Starkey, J., Mansinha, L.: Segmentation of petrographic images by integrating edge detection and region growing. Comput. Geosci. **30**, 817–831 (2004)
22. Marinonia, N., Pavesea, A., Foia, M., Trombinoa, L.: Characterisation of mortar morphology in thin sections by digital image processing. Cem. Concr. Res. **35**, 1613–1619 (2005)
23. Ross, B.J., Fueten, F., Yashkir, D.Y.: Automatic mineral identification using genetic programming. Mach. Vis. Appl. **13**, 61–69 (2001)
24. Plevová, E., Šugárková, V.: Vliv anizotropie a minerálního složení hornin na dilataci hornin. Chemické Listy (2006, in press)
25. Starkey, J., Samantaray, A.K.: Edge detection in petrographic images. J. Microsc. **172**, 263–266 (1993)
26. Goodchild, J.S., Fueten, F.: Edge detection in petrographic images using the rotating polarizer stage. Comput. Geosci. **24**(8), 745–751 (1998)
27. Obara, B.: Application of the image analysis method to the detection of transcrystalline microcracks observed in microscope images of dolomite and granite structures. Arch. Min. Sci. **50**(4), 537–551 (2005)
28. Obara, B.: Application of the image analysis method to the detection of transcrystalline microcracks observed in microscope images of rock structures. Geophys. Res. Abstr. **8**, 16 (2006)
29. Serra, J.: Image analysis and mathematical Morphology. Academic Press, New York (1982)